Author Manuscript

Author Manuscript

Author Manuscript

Author Manuscript

HHS Public Access

Author manuscript

Clin Genitourin Cancer. Author manuscript; available in PMC 2015 March 18.

Published in final edited form as:

Clin Genitourin Cancer. 2014 February ; 12(1): 55–62. doi:10.1016/j.clgc.2013.07.006.

Tumor Necrosis on Magnetic Resonance Imaging Correlates with Aggressive Histology and Disease Progression in Clear Cell Renal Cell Carcinoma

Peter Beddy[1], **Elizabeth M Genega**[2], **Long Ngo**[3], **Nicole Hindman**[4], **Jesse Wei**[1], **Andrea Bullock**[5], **Rupal S Bhatt**[5], **Michael B Atkins**[5,6], and **Ivan Pedrosa**[1,7]

[1]Department of Radiology, St. James Hospital and Trinity College. Dublin, Ireland [2]Department of Pathology, Beth Israel Deaconess Medical Center. Boston, MA [3]Department of Medicine, Beth Israel Deaconess Medical Center. Boston, MA [4]Department of Radiology, New York University Langone Medical Center, New York, NY [5]Department of Medicine, Division of Hematology/ Oncology, Beth Israel Deaconess Medical Center. Boston, MA

Abstract

Purpose—To correlate the magnetic resonance imaging (MRI) features of clear cell renal cell carcinoma (ccRCC) with the histopathological features and disease progression.

Material and Methods—IRB approval for this retrospective study was obtained; patient consent was not required. The initial staging MRIs of 75 patients with histologically confirmed ccRCC were retrospectively reviewed. The imaging was assessed by two radiologists for the presence of tumor necrosis, cystic degeneration, intracellular fat, hemorrhage, retroperitoneal collaterals and renal vein thrombosis. Quantitative analysis for the MRI presence of intracellular lipid within tumors was performed. MRI findings were correlated with histopathologic findings of clear cell percentage, alveolar and tubular growth pattern and disease progression. Statistical associations were evaluated with non-parametric univariable analyses and multivariable logistic regression models.

Results—Correlation between MRI and histopathologic features was performed in 75 patients whereas follow-up data was available for progression analysis in 68 patients. The presence of tumor necrosis, retroperitoneal collaterals and renal vein thrombosis on MRI were significantly associated with low percentage of tumor cells with clear cytoplasm ($p<0.01$) and with metastatic disease at presentation or disease progression ($p<0.01$). At multivariable analysis, necrosis remained as the only feature statistically associated with disease progression ($p=0.03$, adjusted

CORRESPONDING AUTHOR (new institutional address): Ivan Pedrosa, MD, Department of Radiology, University of Texas Southwestern, 5323 Harry Hines Blvd., Dallas, TX 75390-8896, ivan.pedrosa@UTsouthwestern.edu.
[6]Current address: Georgetown Lombardi Comprehensive Cancer Center in Washington, DC.
[7]Current address: University of Texas Southwestern Medical Center. Dallas, TX.

Conflict of Interest

All authors state that they have no conflict of interest

The content is solely the responsibility of the authors and does not necessarily represent the official views of Harvard Catalyst, Harvard University and its affiliated academic health care centers, the National Center for Research Resources, or the National Institutes of Health.

Author Manuscript Author Manuscript Author Manuscript Author Manuscript

odds ratio=27.7, CI 95%=1.4–554.7 for reader one and p=0.02, adjusted odds ratio=29.3, CI 95%=1.7–520.8 for reader two).

Conclusion—Necrosis in ccRCC on MRI correlates with the histopathological finding of lower percentage of tumor cells with clear cytoplasm and is a poor prognostic indicator irrespective of tumor size.

Keywords

MRI; Kidney neoplasms; Carcinoma; Clear-cell metastatic renal cell carcinoma; clear cell percentage

INTRODUCTION

In 2010, an estimated 59,000 Americans were diagnosed with renal cell carcinoma (RCC) and approximately 13,000 died from the disease (1). The different subtypes of RCC and their distinct molecular characteristics (2) has led to improved treatment and therapy directed by tumor subtype (3, 4). Although cytokine therapy with interferon alfa or interleukin-2 (IL-2) was considered as the standard treatment for metastatic RCC (mRCC) prior to the introduction of targeted therapies, the latter are now considered the standard of care for most patients with mRCC.

It has been previously shown that magnetic resonance imaging (MRI) can accurately differentiate RCC histological subtypes based on the dynamic contrast enhancement pattern and the morphological appearance (5, 6). A feature analysis of the appearance of renal masses on conventional T1- and T2-weighted MRI combined with contrast-kinetics on gadolinium-enhanced MRI allows for distinction between the three most common histologic subtypes (i.e. clear cell, papillary, and chromophobe) (5, 6) and angiomyolipomas without visible fat (7) with high degree of diagnostic accuracy. Furthermore, certain MRI characteristics or ‘imaging fenotype’ are predictive of the growth kinetics among different renal masses, which could help predict their aggressiveness (8).

MRI provides also information about the tumor characteristics such as the presence of necrosis or hemorrhage, it can detect intracellular lipids, and delineate intracystic architecture such as nodules or septations (9–11). These morphological MRI features may correlate with the histological appearance of ccRCC and give useful prognostic information about the tumor subtype. The aim of this study was to correlate the MRI features of ccRCC with the pathological features and to assess if the MRI features correlate with disease progression / metastatic disease.

MATERIAL AND METHODS

Study population

This was a single institution, HIPAA-compliant, IRB-approved retrospective study with waiver of informed consent. A computerized MRI database was retrospectively searched from January 2001 to September 2006 for patients with a pre-surgical MRI for assessment of a renal mass and a histologically confirmed diagnosis of ccRCC. First, the study

Author Manuscript Author Manuscript Author Manuscript Author Manuscript

correlated the MRI features of ccRCC with the histological appearance. Patients were excluded if the imaging or pathological specimen were unavailable for review. Then, MRI tumor features were correlated with time to disease progression. Patients were excluded if follow up survival data were unavailable.

Imaging technique

All patients were imaged using on a 1.5T clinical scanner (Vision or Symphony; Siemens Medical Systems, Erlangen, Germany; Excite TwinSpeed or Excite HD; GE Healthcare, Waukesha, WI) with the following sequences; Chemical shift imaging (CSI) with axial dual-echo T1-weighted (T1W) gradient echo (GRE) in phase (IP) and opposed phase (OP) images (repetition time / echo time; 180–205 / 2.2 (OP) – 4.4 (IP) msec, flip angle 80°, 160 × 256 matrix, 1 acquired signals, 35–40-cm field of view, section thickness of 6–8 mm with a gap 1mm and a bandwidth of +/− 62 kHz). Coronal T2-weighted (T2W) half-Fourier single shot fast spin echo (HASTE or SSFSE) was then performed (repetition time / echo time; infinite / 60 msec, flip angle 130–155°, 192×256 matrix, 35–40 cm field of view, section thickness of 4–5 mm with a 1-mm gap and a bandwidth +/− 62 kHz).

Additionally, coronal and sagittal three-dimensional (3D) T1W GRE images (repetition time / echo time; 3.8–4.5 /1.8–2.0 msec, flip angle 12°, 35–45 cm field of view, section thickness of 3–4 mm and a bandwidth +/− 62 kHz) were obtained before and after administration of a bolus of 0.1 mmol/kg body weight of gadopentetate dimeglumine (Magnevist; Berlex Laboratories, Wayne, NJ) at a rate of 2 cc/sec and followed by a 20 cc saline flush. Post contrast coronal images were acquired dynamically in the corticomedullary and nephrographic phases with a first pass timed to the corticomedullary phase using a 2 cc test bolus of gadolinium. The nephrographic phase was initiated 20 seconds after the corticomedullary phase. Post-contrast sagittal 3D T1-W GRE images were acquired during the excretory phase immediately after completion of the dynamic coronal acquisitions.

Quantitative analysis

Region of Interest (ROI) analysis was performed on all lesions to assess for the presence of intracellular lipids in the tumor based on previously validated technique (11–13). Briefly, the technique involved calculation of the change in signal intensity (SI) in the tumor between IP and OP images. The SI index was then calculated as follows: [(tIP – tOP) /(tIP)] × 100, where tIP is tumor SI on IP images, and tOP is tumor SI on OP images. Based on prior experience in adrenal adenomas, intracellular lipid was considered to be present if the SI Index was greater than 16.5% (11–13). The ROI analysis were performed by one radiologist (NH) with 1 year fellowship training in abdominal MRI, 7 months prior to performing the qualitative imaging analysis to avoid recall bias. A circular ROI was placed in the center of the tumor, encompassing at least two thirds of its solid component (average and minimum area size of 9.7 cm^2 and 1.7 cm^2, respectively). The area, location and size of the ROI were constant between IP and OP images. Care was taken to avoid the edge of the tumor, near its interface with the adjacent peri-renal fat, so that phase cancellation artifact could be avoided (14, 15).

Author Manuscript Author Manuscript Author Manuscript Author Manuscript

Qualitative analysis

MR images were analyzed by two radiologists independently (NH, JW, each with 1 year fellowship training in abdominal MRI) to assess for the following attributes in the renal mass: 1) necrosis: high SI on T2W images (but not as high as fluid), low SI on T1W images, lack of enhancement, and central location within the tumor; 2) cystic degeneration: areas with very high SI on T2W images (similar to that of fluid elsewhere), low SI on T1W images, lack of enhancement, and lobulated cystic morphology; 3) the presence or absence of intravoxel fat (subjective loss of SI on OP images relative to IP images); 4) hemorrhage: non-enhancing areas of high SI on T1W and variable signal on T2W; 5) retroperitoneal collateral vessels; 6) renal vein thrombosis (9, 16). Tumor size was also measured for each tumor and the longest dimension was recorded.

Progression Analysis

A retrospective review of the electronic medical record was performed on all patients by a single reviewer (AB) who was unaware of the MRI findings. Data collected included standard patient and disease characteristics, baseline laboratory and biochemical parameters, disease stage at presentation and time to progression. The presence of disease progression was defined as radiological evidence of tumor recurrence or metastases after nephrectomy or metastatic disease at presentation.

Pathology Analysis

All slides for each tumor were reviewed to confirm the clear cell histology by a single uropathologist with 11 years of experience (EMG). Slides were evaluated for the following pathologic features: 1) tumor grade; 2) percentage of tumor cells with clear cytoplasm in each tumor; 3) percentage of tumor cells with granular eosinophilic cytoplasm in each tumor; 4) percentage of tumor with alveolar growth (compact, relatively small nests/acini each surrounded by delicate fibrovascular septae; and 5) percentage of tumor with tubular growth (circular arrangement of tumor cells [gland-like] with a central space).

Statistical Analysis

Univariable analysis was used to examine the association between pathologic and MRI features. Since the distribution of the pathologic features (e.g. clear cell percentage) was asymmetric, a nonparametric median test was used to assess the difference in the medians between those with the MRI feature and those without. The statistically significant (p-values ≤ 0.05) features were then entered into a multivariable model. MRI features associated with progression were identified with a Fisher's exact test and then entered into a multivariable logistic regression model. Since there were cells with zeros, quasi-complete separation problem occurred which required the use of the Firth's correction factor in the logistic regression model (17). Kappa statistic was used to assess the inter-reader variability for both reviewers (≥ 0.6 = good agreement). All statistical analyses were carried out with SAS software (18)

Author Manuscript Author Manuscript Author Manuscript Author Manuscript

RESULTS

Patients

Seventy-five patients were included in the study (53 men and 22 woman; mean age 58.2 years, range 25–88 years). Sixty-eight patients (follow-up cohort) had data available for assessment of disease progression (48 men and 20 woman; mean age 57.7 years, range 27–88 years). Patient characteristics are included in Table 1.

Pathological diagnosis

Pathological diagnosis was achieved by radical nephrectomy (n=42), partial nephrectomy (n=29), or percutaneous core biopsy (n=4). Mean tumor size was 5.5 cm (range 1.1–19.7 cm) for all patients and 5.6 cm (range 1.1–19.7 cm) for the follow-up cohort. Mean percentages per tumor of tumor cells with clear cytoplasm, alveolar growth, and tubular growth at histopathology were 63.1% (range 0–100), 42.8% (range 0–100), and 23.1% (range 0–100) for all patients and 61.8% (range 0–100), 43.5% (range 0–100), and 25.0% (range 0–100) for the follow-up cohort, respectively.

Quantitative analysis

There was no association between the MRI SI index ($p=0.93$) and the percentage clear cells at histopathology (Figure 1).

Qualitative analysis

Tumors with MRI evidence of necrosis, retroperitoneal collateral vessels, and renal vein thrombosis had a significantly lower percentage of tumor cells with clear cytoplasm ($p<0.001$) (Table 2). There was no association between the percentage of clear cells and the MRI presence of cystic degeneration, hemorrhage, or intracellular fat. Intracellular lipids were associated with percentage of alveolar growth for reader 1 ($p=0.03$) but not for reader 2. The other MRI features were not associated with percentage of alveolar growth. MRI features were not associated with percentage of tubular growth. There was a high level of inter-observer agreement in assessing MRI evidence of necrosis (kappa=0.97), intracellular lipids (kappa=0.60), retroperitoneal collaterals (kappa=0.94) and renal vein thrombosis (kappa=0.80).

Disease Progression

Sixteen patients in the follow-up cohort (n=68) progressed during the study period, 15 of these with metastases and 1 with local recurrence (Table 3). Eleven had distant metastases (progression) at presentation whereas 5 patients develop metastasis or local recurrence in the follow up period. The mean time to progression was 244 days (range 0–1381). The mean follow up time in those who did not progress was 2012 days (range 1095–2890 days).

Tumor size, grade and stage were statistically associated with progression or metastatic disease ($p<0.0001$)(Table 3). The mean tumor size for patients with disease progression or metastasis at presentation was 9.8 cm (range 4–19.7 cm), the mean tumor size for patients without progression or metastasis at presentation was 4.3 cm (range 1.1–15 cm).

Author Manuscript Author Manuscript Author Manuscript Author Manuscript

Both clear cytoplasm and tubular growth at histopathology were associated with disease progression or metastases (Table 3). The median clear cell and tubular percentage at histopathology was significantly lower ($p < 0.001$ and $p = 0.02$, respectively) in patients that exhibit progression / metastasis at presentation. There was no association between percentage of alveolar growth and disease progression.

MRI evidence of necrosis, retroperitoneal collaterals, and renal vein thrombosis were associated with disease progression or metastatic disease at presentation ($p<0.0001$) (Figure 2). Furthermore, all patients who progressed had necrosis on MRI. At multivariable logistic regression analysis, including MRI features, tumor size, grade, and stage, only necrosis remained statistically associated with progression or metastasis ($p=0.03$, adjusted odds ratio=27.7, CI 95%=1.4–554.7 for reader one and $p=0.02$, adjusted odds ratio=29.8, CI 95%=1.7–520.8 for reader two). Detection of tumor necrosis on MRI was highly reproducible with virtually perfect agreement between both reviewers (Kappa statistic 0.97).

DISCUSSION

This study demonstrates that tumors with MRI evidence of necrosis, retroperitoneal collateral vessels and renal vein thrombosis had a significantly lower pathological percentage of tumor cells with clear cytoplasm than tumors without these MRI features. ccRCC with a high percentage of cells with clear cytoplasm have been previously shown to have a more favorable prognosis than those with a relatively low or absent clear cell component (19). The tumors with necrosis on MRI not only had a lower clear cell percentage but also were significantly more likely to have disease progression or metastatic disease at presentation compared to tumors that did not have necrosis. No patient had disease progression during the study if necrosis was absent on the initial MRI, regardless of the tumor size at presentation. The finding of tumor necrosis on MRI was also extremely reliable with near perfect agreement between the two readers in the study (Kappa 0.97).

The influence of tumor size on progression was also analyzed and as one might expect, larger tumors tend to have more necrosis. Patients with larger tumors are more likely to have metastases at presentation and progress earlier than patients with smaller tumor. Similarly a higher Fuhrman grade and stage at presentation correlated with disease progression. Multivariate analysis of tumor size, grade, stage and the MRI features associated with progression demonstrated however that only necrosis remained significantly associated with poor prognosis. MRI evidence of necrosis was strongly predictive of disease progression irrespective of size. Tumor necrosis at histopathology correlates with a worse prognosis after nephrectomy in patients with ccRCC (20–22). However, the prospective evaluation of necrosis on a presence or absence basis does not provide independent prognostic information (23). In contrast, scoring of necrosis according to its extent with further sub-classification based on a 20% cutoff is an independent prognostic factor (23). Furthermore, tumor necrosis in RCC is more likely induced by acute hypoxia due to immature microvessels (24). An increased number of immature (expressing CD31 but not CD34) than mature (expressing both CD31 and CD34) microvessels is associated with shorter patient survival, higher-grade tumors, and more advanced primary tumors (24).

Author Manuscript Author Manuscript Author Manuscript Author Manuscript

Accurate prognostic information is essential to enable appropriate therapeutic management of ccRCC. Traditional approaches relied on clinical and pathological information, such as overall stage, histological grade and performance status (25–27). Recent molecular characterization has identified markers such as carbonic anhydase IX and B7H1 as powerful predictors of renal tumor response and long term survival (28). Moreover, cytokine therapy is still used some patients because of the potential benefits of achieving a durable complete response (19). Analysis of patients with ccRCC in the Cytokine Working Group clinical trials has shown significant difference in response rates to IL-2 based on tumor histologic appearance (19). Tumors with alveolar growth and the absence of papillary architecture or granular eosinophilic cytoplasm (i.e. high percentage of tumor cells with clear cytoplasm) have been shown to have a significantly higher response rates to IL-2 therapy when compared with tumors with poor prognostic features (i.e. high percentage of cells with granular cytoplasm or papillary features / low clear cell percentage). These observations may allow tailoring of IL-2 treatment to patients with favorable histological features and avoid unnecessary side effects and cost in patients with little chance of response (29).

Our data indicates that in patients with ccRCC, necrosis demonstrated on MR is a strong predictor disease progression (Figure 2). MR imaging evidence of necrosis correlates closely with a low clear cell percentage on histology. Thus, it is possible that necrosis on MR imaging may be associated with reduced response rate to IL-2 therapy although the role of this MR finding as a marker for deciding on appropriate treatment for a patient presenting with ccRCC requires further investigation.

The presence of abundant intracytoplasmic glycogen and lipids accounts for the ‘clear’ appearance of the cytoplasm in clear cell RCC (30). Intracellular lipids can be recognized in up to 49% of RCC with clear cell histology using chemical-shift imaging, a standard acquisition included in most clinical MRI protocols (11, 31). We hypothesized that the amount of intracellular lipids at MR imaging, as measured by the SI index, would be predictive of the percentage of clear cell component in the same tumor at histopathology. There was however no such correlation likely indicating that the intracellular accumulation of glycogen and lipids may not occur in parallel.

The study has limitations; no attempt was made to correlate MRI evidence of necrosis with pathological necrosis. However, the appearance of necrosis is well documented on MRI and has previously been shown to correlate closely with bulk necrosis within tumors (9, 16). The perfect interobserver agreement observed also suggests that necrosis on MR imaging has a well-established appearance and is a highly reliable finding. The presence of tumor necrosis on MRI likely correlates with bulk necrosis within the tumor, which would be apparent on the gross-specimen, rather than microscopic necrosis, which would be measured at histopathology. The retrospective nature of this study did not allowed for correlation with bulk tumor necrosis as this is not routinely reported and/or measured at our institution. The definition of progression in the study included those that had metastases at presentation and those who progressed at a later date. Unfortunately, the cohort with delayed progression was too small to evaluate separately.

Author Manuscript Author Manuscript Author Manuscript Author Manuscript

Conclusion

This study demonstrated that the unique morphological features of clear cell renal cell carcinoma on MRI closely correlate with the percentage of clear cell features in the tumor at histopathology. MRI evidence of necrosis, retroperitoneal collaterals and renal vein thrombosis were poor prognostic indicators in our patient cohort and necrosis was associated with disease progression irrespective of tumor size. The findings in our study may help in therapeutic management as patients with a poor prognostic tumor can be detected on their initial staging MRI. Future correlation between the MRI features and molecular markers such as carbonic anhydase IX and B7H1 could refine MRI as a prognostic tool for renal cell carcinoma.

Acknowledgments

Funding source

This work was conducted with support from Harvard Catalyst/ The Harvard Clinical and Translational Science Center (NIH Award #UL1 RR 025758 and financial contributions from Harvard University and its affiliated academic health care centers).

References

1. National Cancer Institute. Cancer Stat Fact Sheets: cancer of the kidney and renal pelvis. [cited 2010 December 28]; Available from: http://seer.cancer.gov/statfacts/html/kidrp.html
2. McDermott DF. Immunotherapy of metastatic renal cell carcinoma. Cancer. 2009 May 15; 115(10 Suppl):2298–305. [PubMed: 19402060]
3. Schrader AJ, Olbert PJ, Hegele A, Varga Z, Hofmann R. Metastatic non-clear cell renal cell carcinoma: current therapeutic options. BJU Int. 2008 Jun; 101(11):1343–5. [PubMed: 18241246]
4. Motzer RJ, Hutson TE, Tomczak P, Michaelson MD, Bukowski RM, Rixe O, et al. Sunitinib versus interferon alfa in metastatic renal-cell carcinoma. N Engl J Med. 2007 Jan 11; 356(2):115–24. [PubMed: 17215529]
5. Sun MR, Ngo L, Genega EM, Atkins MB, Finn ME, Rofsky NM, et al. Renal cell carcinoma: dynamic contrast-enhanced MR imaging for differentiation of tumor subtypes--correlation with pathologic findings. Radiology. 2009 Mar; 250(3):793–802. [PubMed: 19244046]
6. Pedrosa I, Chou MT, Ngo L, RHB, Genega EM, Galaburda L, et al. MR classification of renal masses with pathologic correlation. Eur Radiol. 2008 Feb; 18(2):365–75. [PubMed: 17899106]
7. Sasiwimonphan K, Takahashi N, Leibovich BC, Carter RE, Atwell TD, Kawashima A. Small (<4 cm) renal mass: differentiation of angiomyolipoma without visible fat from renal cell carcinoma utilizing MR imaging. Radiology. 2012 Apr; 263(1):160–8. [PubMed: 22344404]
8. Dodelzon K, Mussi TC, Babb JS, Taneja SS, Rosenkrantz AB. Prediction of growth rate of solid renal masses: utility of MR imaging features--preliminary experience. Radiology. 2012 Mar; 262(3):884–93. [PubMed: 22267588]
9. Pedrosa I, Sun MR, Spencer M, Genega EM, Olumi AF, Dewolf WC, et al. MR imaging of renal masses: correlation with findings at surgery and pathologic analysis. Radiographics. 2008 Jul-Aug; 28(4):985–1003. [PubMed: 18635625]
10. Choudhary S, Sudarshan S, Choyke PL, Prasad SR. Renal cell carcinoma: recent advances in genetics and imaging. Semin Ultrasound CT MR. 2009 Aug; 30(4):315–25. [PubMed: 19711643]
11. Outwater EK, Bhatia M, Siegelman ES, Burke MA, Mitchell DG. Lipid in renal clear cell carcinoma: detection on opposed-phase gradient-echo MR images. Radiology. 1997 Oct; 205(1): 103–7. [PubMed: 9314970]
12. Israel GM, Korobkin M, Wang C, Hecht EN, Krinsky GA. Comparison of unenhanced CT and chemical shift MRI in evaluating lipid-rich adrenal adenomas. AJR Am J Roentgenol. 2004 Jul; 183(1):215–9. [PubMed: 15208141]

Author Manuscript Author Manuscript Author Manuscript Author Manuscript

13. Outwater EK, Blasbalg R, Siegelman ES, Vala M. Detection of lipid in abdominal tissues with opposed-phase gradient-echo images at 1.5 T: techniques and diagnostic importance. Radiographics. 1998 Nov-Dec;18(6):1465–80. [PubMed: 9821195]
14. Hood MN, Ho VB, Smirniotopoulos JG, Szumowski J. Chemical shift: the artifact and clinical tool revisited. Radiographics. 1999 Mar-Apr;19(2):357–71. [PubMed: 10194784]
15. Delfaut EM, Beltran J, Johnson G, Rousseau J, Marchandise X, Cotten A. Fat suppression in MR imaging: techniques and pitfalls. Radiographics. 1999 Mar-Apr;19(2):373–82. [PubMed: 10194785]
16. Hammoud MA, Sawaya R, Shi W, Thall PF, Leeds NE. Prognostic significance of preoperative MRI scans in glioblastoma multiforme. J Neurooncol. 1996 Jan; 27(1):65–73. [PubMed: 8699228]
17. Firth D. Bias Reduction of Maximum Likelihood Estimates. Biometrika. 1993; 80:27–38.
18. SAS Institute Inc. SAS/STAT Software. 8. Cary NC: 2003.
19. Upton MP, Parker RA, Youmans A, McDermott DF, Atkins MB. Histologic predictors of renal cell carcinoma response to interleukin-2-based therapy. J Immunother. 2005 Sep-Oct;28(5):488–95. [PubMed: 16113605]
20. Frank I, Blute ML, Cheville JC, Lohse CM, Weaver AL, Zincke H. An outcome prediction model for patients with clear cell renal cell carcinoma treated with radical nephrectomy based on tumor stage, size, grade and necrosis: the SSIGN score. J Urol. 2002 Dec; 168(6):2395–400. [PubMed: 12441925]
21. Minardi D, Lucarini G, Filosa A, Milanese G, Zizzi A, Di Primio R, et al. Prognostic role of tumor necrosis, microvessel density, vascular endothelial growth factor and hypoxia inducible factor-1alpha in patients with clear cell renal carcinoma after radical nephrectomy in a long term follow-up. Int J Immunopathol Pharmacol. 2008 Apr-Jun;21(2):447–55. [PubMed: 18547492]
22. Sengupta S, Lohse CM, Leibovich BC, Frank I, Thompson RH, Webster WS, et al. Histologic coagulative tumor necrosis as a prognostic indicator of renal cell carcinoma aggressiveness. Cancer. 2005 Aug 1; 104(3):511–20. [PubMed: 15973740]
23. Klatte T, Said JW, de Martino M, Larochelle J, Shuch B, Rao JY, et al. Presence of tumor necrosis is not a significant predictor of survival in clear cell renal cell carcinoma: higher prognostic accuracy of extent based rather than presence/absence classification. J Urol. 2009 Apr; 181(4): 1558–64. discussion 63–4. [PubMed: 19230920]
24. Hemmerlein B, Kugler A, Ozisik R, Ringert RH, Radzun HJ, Thelen P. Vascular endothelial growth factor expression, angiogenesis, and necrosis in renal cell carcinomas. Virchows Arch. 2001 Nov; 439(5):645–52. [PubMed: 11764385]
25. Motzer RJ, Bacik J, Murphy BA, Russo P, Mazumdar M. Interferon-alfa as a comparative treatment for clinical trials of new therapies against advanced renal cell carcinoma. J Clin Oncol. 2002 Jan 1; 20(1):289–96. [PubMed: 11773181]
26. Kattan MW, Reuter V, Motzer RJ, Katz J, Russo P. A postoperative prognostic nomogram for renal cell carcinoma. J Urol. 2001 Jul; 166(1):63–7. [PubMed: 11435824]
27. Zisman A, Pantuck AJ, Wieder J, Chao DH, Dorey F, Said JW, et al. Risk group assessment and clinical outcome algorithm to predict the natural history of patients with surgically resected renal cell carcinoma. J Clin Oncol. 2002 Dec 1; 20(23):4559–66. [PubMed: 12454113]
28. Atkins MB, Bukowski RM, Escudier BJ, Figlin RA, Hudes GH, Kaelin WG Jr, et al. Innovations and challenges in renal cancer: summary statement from the Third Cambridge Conference. Cancer. 2009 May 15; 115(10 Suppl):2247–51. [PubMed: 19402064]
29. McDermott DF, Atkins MB. Interleukin-2 therapy of metastatic renal cell carcinoma--predictors of response. Semin Oncol. 2006 Oct; 33(5):583–7. [PubMed: 17045087]
30. Krishnan B, Truong LD. Renal epithelial neoplasms: the diagnostic implications of electron microscopic study in 55 cases. Hum Pathol. 2002 Jan; 33(1):68–79. [PubMed: 11823975]
31. Hindman N, Ngo L, Genega EM, Melamed J, Wei J, Braza JM, et al. Angiomyolipoma with minimal fat: can it be differentiated from clear cell renal cell carcinoma by using standard MR techniques? Radiology. 2012 Nov; 265(2):468–77. [PubMed: 23012463]

Author Manuscript Author Manuscript Author Manuscript Author Manuscript

Clinical Practice Points

- MRI can differentiate the subtypes of RCC based on the morphological appearance and enhancement pattern. This study demonstrates that ccRCC with MRI evidence of necrosis, retroperitoneal collateral vessels and renal vein thrombosis have a lower pathological percentage of tumor cells with clear cytoplasm than tumors without these MRI features. ccRCCs with necrosis on MRI are significantly more likely to have disease progression or metastatic disease at presentation compared to tumors that do not have necrosis irrespective of the size of the tumor.
- MRI evidence of necrosis on an initial staging study is a poor prognostic indicator and may be helpful in guiding therapeutic management. Patients with MRI evidence of necrosis, retroperitoneal collaterals and renal vein thrombosis have a lower pathological percentage of tumor cells with clear cytoplasm and may be less likely to respond to IL2 therapy.

Author Manuscript Author Manuscript Author Manuscript Author Manuscript

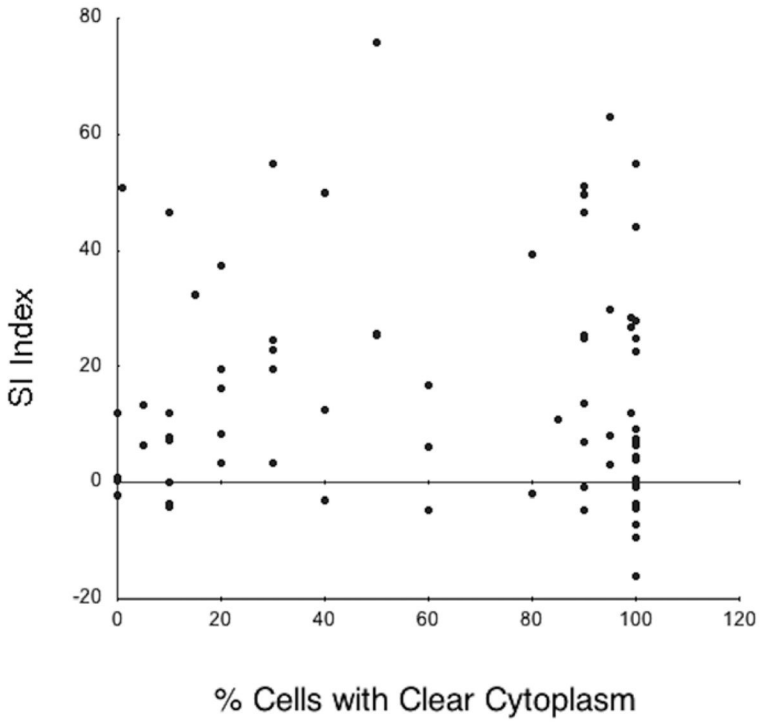

Figure 1.

Correlation between percentage of tumor cells with clear cytoplasm and the signal intensity index. There was no statistical association (p=0.93) between these two variables indicating lack of correlation between intracellular lipids on MRI and clear cytoplasms at histopathology.

Author Manuscript Author Manuscript Author Manuscript Author Manuscript

Figure 2A

Figure 2B

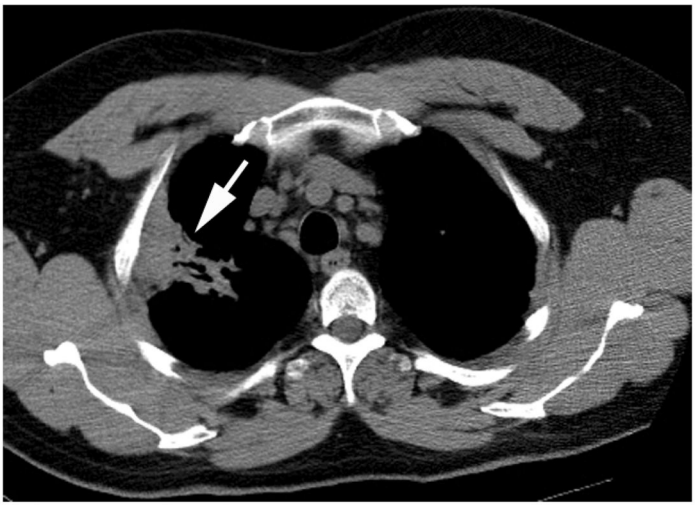

Author Manuscript Author Manuscript Author Manuscript Author Manuscript

Figure 2C

Figure 2.

Thirty-eight year-old male with history of sarcoidosis and left renal mass. A) Gadolinium-enhanced coronal T1-weighted gradient echo MR image shows a 6.5 cm mass in the upper pole of the left kidney. A central non-enhancing area of necrosis is present (black arrow). Multiple enlarged retroperitoneal lymph nodes (arrowheads) are also seen. After nephrectomy, histopathology analysis revealed clear cell carcinoma, Fuhrman grade II. Analysis of the retroperitoneal lymph nodes demonstrated numerous non-necrotizing granulomas but no evidence of metastatic disease. B) Axial CT image of the chest obtained 1 year after nephrectomy shows stable lung parenchymal consolidation in the right upper pole (arrow) compared to prior CT examinations (not shown) consistent with sarcoidosis. C) Axial contrast-enhanced CT at the same level as B, obtained 3 years after nephrectomy, shows persistent lung consolidation (arrow) and a new enhancing soft tissue nodule in the subcutaneous fat of the back (arrowhead). Histopathologic evaluation of this soft-tissue nodule after surgical excision confirmed metastatic clear cell renal cell carcinoma

Author Manuscript Author Manuscript Author Manuscript Author Manuscript

Table 1

Patient characteristics (N=75)

		Range
Median Age	59	(25–88)
Sex		%
M	53	70
F	22	30
Stage		
I	48	63
II	11	16
III	1	1
IV	12	16
N/A	2	3
Grade		
I	8	11
II	43	55
III	16	22
IV	5	7
N/A	3	4
Histology		
Clear Cell	75	100

Author Manuscript Author Manuscript Author Manuscript Author Manuscript

Table 2

Association between MRI features and percentages of tumor cells with clear cell cytoplasm, alveolar growth, and tubular growth * statistically significant at type-I error of 0.05 using nonparametric median test

	MRI Feature		n	Clear Cell Percentage				Alveolar Percentage				Tubular Percentage			
				Mean	Median	SD	p-value	Mean	Median	SD	p-value	Mean	Median	SD	p-value
R1	Necrosis	Y	28	39.8	25.0	35.4	<0.001*	40.9	25.0	39.1	0.70	17.7	10.0	26.5	0.60
		N	47	77.0	95.0	33.6		43.9	45.0	42.1		26.4	10.0	33.0	
R2	Necrosis	Y	29	38.8	20.0	35.2	<0.001*	39.5	25.0	39.2	0.54	18.1	10.0	26.1	0.80
		N	46	78.5	97.0	32.5		44.9	45.0	42.1		26.3	10.0	33.4	
	Kappa=0.97														
R1	Microscopic fat	Y	35	63.5	90.0	38.5	0.93	54.1	70.0	40.6	0.03*	24.6	10.0	33.1	0.70
		N	40	62.7	85.0	39.3		32.9	10.0	38.7		21.9	10.0	29.1	
R2	Microscopic fat	Y	40	58.5	60	37.6	0.12	51.4	64.0	41.1	0.13	18.4	5.0	27.9	0.07
		N	35	68.4	90	39.7		33.0	10.0	38.7		28.6	10.0	33.4	
	Kappa=0.60														
R1	Retroperitoneal collaterals	Y	29	36.7	20.0	34.6	<0.001*	46.5	30.0	40.8	0.37	10.9	5.0	16.5	0.10
		N	46	79.8	95.0	31.2		40.4	17.0	41.0		30.9	10.0	35.2	
R2	Retroperitoneal collaterals	Y	29	37.9	30.0	34.1	<0.001*	46.7	30.0	40.6	0.74	12.6	5.0	18.9	0.14
		N	46	79.0	95.0	32.6		40.3	17.0	41.1		39.8	10.0	35.0	
	Kappa=0.94														
R1	Renal vein thrombosis	Y	10	22.0	15.0	21.9	<0.001*	43.5	22.5	43.2	0.52	5.0	0.0	8.2	0.056
		N	65	69.4	90.0	36.8		42.7	30.0	40.8		25.9	10.0	32.1	
R2	Renal vein thrombosis	Y	7	17.1	5.0	22.0	<0.01*	46.4	25.0	45.0	0.72	5.0	0.0	9.6	0.12
		N	68	67.8	90.0	36.9		42.4	27.5	40.7		25.0	10.0	31.7	
	Kappa=0.80														

R1= Reviewer 1; R2=Reviewer 2.

Author Manuscript Author Manuscript Author Manuscript Author Manuscript

Clin Genitourin Cancer. Author manuscript; available in PMC 2015 March 18.

Table 3

Association between MRI and pathological features and disease progression

	MRI Feature		Progression n=68		P-value from Fisher's exact test
			Yes	No	
R1	Necrosis	Yes	16	11	<0.0001*
		No	0	41	
R2	Necrosis	Yes	16	11	<0.0001*
		No	0	41	
R1	Microscopic fat	Yes	7	27	0.78
		No	9	25	
R2	Microscopic fat	Yes	11	28	0.39
		No	5	24	
R1	Retroperitoneal Collaterals	Yes	15	12	<0.0001*
		No	1	40	
R2	Retroperitoneal Collaterals	Yes	14	13	<0.0001*
		No	2	39	
R1	Renal vein thrombosis	Yes	8	1	<0.0001*
		No	8	51	
R2	Renal vein thrombosis	Yes	6	0	<0.0001*
		No	10	52	

		Progression		P-value from nonparametric median test
		Yes	No	
	Pathological Feature			
	Clear cell percentage	21.3	74.3	<0.0001*
	Alveolar percentage	36.8	45.6	0.57
	Tubular percentage	5.1	30.8	0.02*
	Fuhrman Grade			<0.0001*
	1	0	7	
	2	4	32	

Author Manuscript Author Manuscript Author Manuscript Author Manuscript

		Progression		P-value from nonparametric median test
		Yes	No	
	3	5	7	
	4	5	4	
Stage				<0.0001*
	1	2	41	
	2	2	7	
	3	1	0	
	4	12	0	

* statistically significant at type-I error of 0.05